J Mater Sci (2014) 49:3805–3815
DOI 10.1007/s10853-014-8092-8

Effects of zinc on the interfacial reactions of tin–indium solder joints with copper

Shih-Kang Lin · Ru-Bo Chang · Sinn-Wen Chen · Ming-Yueh Tsai · Chia-Ming Hsu

Received: 24 November 2013 / Accepted: 29 January 2014 / Published online: 13 February 2014

Abstract Sn-20.0 wt%In (Sn-20.0In) alloy is a promising base material in Pb-free solders for low-temperature applications. Zn is often used as an additive to Pb-free solders to reduce the extent of undercooling during reflow. Cu is the most commonly used substrate in electronics industry. Interfacial stability at Sn–In–Zn/Cu joints is crucial to reliability of electronic products. In this study, interfacial reactions between Sn-20.0 wt%In-x wt%Zn (Sn-20.0In-xZn) solders and Cu where $x = 0.5$, 0.7, 1.0, 2.0, 3.0, and 5.0 at 150, 230, and 260 °C were experimentally examined. It is found that the reaction phase formation and interfacial morphologies are strongly influenced by Zn concentrations. The reaction phases evolve from the Cu_6Sn_5 phase, CuZn and Cu_5Zn_8 phase, to Cu_5Zn_8 phase with higher Zn doping in the solders. The Cu_5Zn_8 phase acted as a diffusion barrier and suppressed the growth of the Cu_6Sn_5 phase. The results indicate that 2.0 wt%Zn addition resulted in the gentlest reactions during both soldering and solid-state ageing in Sn-20.0In-xZn/Cu couples.

S.-K. Lin · M.-Y. Tsai
Department of Materials Science and Engineering, National Cheng Kung University, Tainan 701, Taiwan

S.-K. Lin
Promotion Center for Global Materials Research, National Cheng Kung University, Tainan 701, Taiwan

S.-K. Lin
Center for Micro/Nano Science and Technology, National Cheng Kung University, Tainan 701, Taiwan

R.-B. Chang · S.-W. Chen (✉)
Department of Chemical Engineering, National Tsing Hua University, Hsinchu 300, Taiwan
e-mail: swchen@mx.nthu.edu.tw

C.-M. Hsu
Department of Chemical Engineering, National United University, Miaoli 360, Taiwan

Introduction

Soldering is the key step in various interconnection technologies including tape-automated bonding (TAB), flip chip-ball grid array (FC-BGA) packaging, and the more recent three-dimensional integrated circuit (3D IC) packaging in electronics industry [1, 2]. Reliable solder joints ensure the required lifetime of electronic products, while uncontrolled interfaces at solder joints can raise significant reliability concerns. Conventional eutectic Pb–Sn solder has been banned for consumer electronic products due to the prominent neural toxicity of Pb [3]. In the past decade, extensive efforts have been devoted to developing alternative Pb-free solders [1, 2, 4–6]. The Sn–In binary alloys, particularly the Sn-20.0 wt%In alloy, have been regarded as a base-alloy for low-temperature applications [7–14]. Zn is a frequently used additive to Pb-free solders. It can reduce the extent of undercooling of Pb-free solders [15, 16]. Cu is the most commonly used substrate materials in electronic packaging. The effects of Zn addition on interfacial reactions of Sn-20.0 wt%In-x wt%Zn (Sn-20In-xZn, $x = 0.5$, 0.7, 1.0, 2.0, 3.0, and 5.0) solders with Cu substrates at 150, 230, and 260 °C are examined in this study. Extremely sensitive responses of reaction phase formation, interfacial microstructure evolution, and reaction kinetics due to minor Zn additions are reported and discussed.

Experimental Procedures

Sn-20In-*x*Zn ($x = 0.5$, 0.7, 1.0, 2.0, 3.0, and 5.0) alloys were prepared from pure Sn (99.98 %, Showa, Japan), pure In (99.9 %, Showa, Japan), and pure Zn (99.9 %, Showa, Japan). Proper amounts of constituent elements were cleaned, precisely weighed, and encapsulated in quartz tubes under a 10^{-2} mbar vacuum. The capsules were annealed at 600 °C for a week to ensure homogeneity of alloys. After heat treatments, the capsules were quenched in icy water. The alloys were then sectioned into 2-g-weight ingots by a diamond saw. A 500-μm-thick pure Cu foil (99.98 %, Sigma-Aldrich, USA) was cut into 5 mm by 8 mm pieces and then metallographically ground and polished down to 0.3 μm Al_2O_3 powders. Each Cu substrate was coated with a thin layer of flux (water soluble, MEC-W-2326, MEC, Taiwan) and encapsulated together with the Sn-20In-*x*Zn solder ingot in quartz tubes under a 10^{-2} mbar vacuum. The capsules were annealed at 150, 230, and 260 °C for predetermined lengths of reaction time. At 230 and 260 °C, the Sn-20In-*x*Zn/Cu reactions were liquid/solid (L/S) reactions. The L/S capsules were quenched in icy water at the end of reactions. However, the reactions at 150 °C were solid/solid (S/S) reactions. Prior to the heat treatments at 150 °C, the couples were prepared with a 30-s reflow process at 230 °C. After reactions, the couples were also quenched in icy water. The resultant couples were analyzed metallographically with a scanning electron microscope (SEM) (JEOL JSM5600, Tokyo, Japan). The compositions of the reaction phases were determined using electron probe microanalysis (EPMA) (JEOL JXA-8200SX, Tokyo, Japan). Pure elements were used as the standard specimens for calibration and the standard ZAF scheme was used for correcting the quantitative measurements in the EPMA. The thicknesses of the intermetallic compounds (IMCs) were measured with an image-processing-software (ImageJ, USA).

Results

Interfacial reactions in Sn-20In-*x*Zn/Cu couples reacted at 230 °C

Figure 1a–e shows the backscattered electron image (BEI) micrographs of the Sn-20In-0.5Zn/Cu and Sn-20In-1.0Zn/Cu couples reacted at 230 °C for 30 min, and of Sn-20In-1.0Zn/Cu, Sn-20In-2.0Zn/Cu, and Sn-20In-3.0Zn/Cu couples reacted at 230 °C for 2 h, respectively. As shown in Fig. 1a, a scallop-type intermetallic layer was observed at the interface. The composition of the interfacial layer was determined to be Sn-55.6 at.%Cu-7.0 at.%In-6.0 at.%Zn. Since the major constituents are Cu and Sn, the phase equilibria of the Cu–In–Sn and Cu–Sn–Zn ternary systems were considered. According to the 250 °C isothermal sections of both Cu–In–Sn [17] and Cu–Sn–Zn [18] ternary systems, Cu–Sn and Cu–In binary phases have large mutual solubility between In and Sn, while there are about 6 and 10 at.% Zn solubility in Cu_6Sn_5 and Cu_3Sn phases, respectively. Moreover, as the Cu–Sn phase regions in both Cu–In–Sn and Cu–Sn–Zn systems are approximately in parallel with the In–Sn and Sn–Zn binary boundaries, i.e., the Cu compositions remain unchanged in the homogeneity ranges of these ternary Cu–Sn compounds [17, 18], In and Zn atoms are likely to substitute the Sn atoms in the ternary Cu–Sn phases. As a result, the quaternary phase with 55.6 at.%Cu is presumed to be the Cu_6Sn_5 phase with 7.0 at.%In and 6.0 at.%Zn. Similar results were found in 0.7 wt%Zn-doped couples. Only a scallop-type Cu_6Sn_5 phase with 9 at.%In and 6.4 at.%Zn was observed at the interface. The Cu_6Sn_5 layers in both couples grew thicker and ripened with increasing reaction time. The reaction paths across the interfaces in 0.5 and 0.7 wt%Zn-doped couples are liquid/Cu_6Sn_5/Cu at 230 °C.

As shown in Fig. 1b, the interfacial morphology changed when the Zn doping level was increased to 1.0 wt%. Instead of the scallop-type layer, a loose reaction layer with fine grains was observed at the interface. Its composition was determined to be Cu-64.8 at.% Zn without detectable In or Sn content. According to the Cu–Zn binary phase diagram [19], the phase is presumed to be the Cu_5Zn_8 phase. As shown in Fig. 1c, the loose Cu_5Zn_8 layer became denser after a 2-h reaction. Similar results were found in Sn-20In-2.0Zn/Cu and Sn-20In-3.0Zn/Cu couples. As shown in Fig. 1d and e, planar reaction layers were formed at the interfaces. The compositions of the layers were determined to be Cu-66.0 at.%Zn and Cu-66.5 at.%Zn, respectively. Both of them are presumed to be the Cu_5Zn_8 phase, same as those formed in Sn-20In-1.0Zn/Cu couples. In addition, since Zn is the major constituent in the solder that participated in the reactions in these couples, faster reaction-progressions were expected for the couples with higher Zn doping levels, which resulted in formation of thicker and flatter reaction layers, as shown in Fig. 1c–e.

In summary, when the doping level of Zn $\leq$ 0.7 wt% in the Sn-20In-*x*Zn/Cu couples reacted at 230 °C, the reaction product is the Cu_6Sn_5 phase. On the other hand, when the Zn content $\geq$1.0 wt%, the Cu_5Zn_8 phase would form at the interface. The reaction products in the Sn-20In-*x*Zn/Cu couples at 230 °C are summarized in Table 1.

Interfacial reactions in Sn-20 In-*x*Zn/Cu couples reacted at 260 °C

Figure 2a–e shows the BEI micrographs of Sn-20In-0.7Zn/Cu couple reacted at 260 °C for 2 h, and of Sn-20In-1.0Zn/

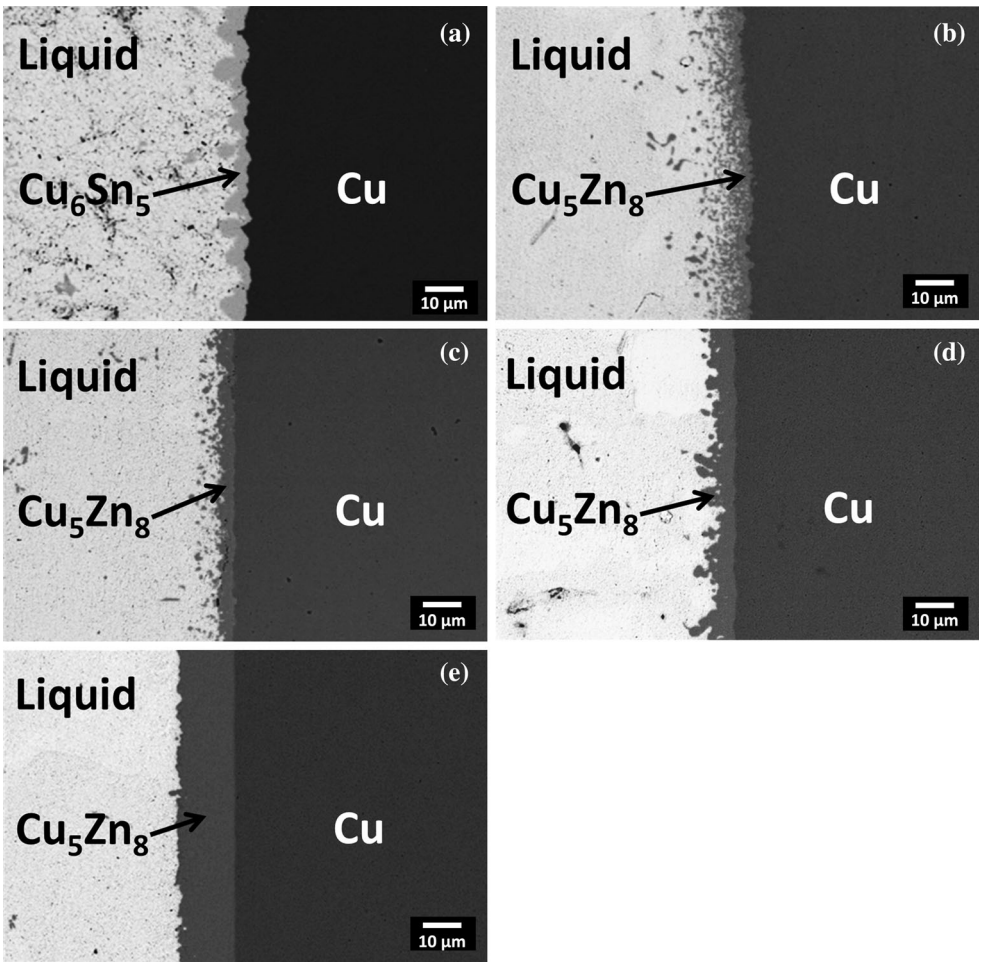

Fig. 1 BEI micrographs of the Sn-20In-*x*Zn/Cu couples reacted at 230 °C: **a** $x = 0.5$ for 30 min, **b** $x = 1.0$ for 30 min, **c** $x = 1.0$ for 2 h, **d** $x = 2.0$ for 2 h, and **e** $x = 3.0$ for 2 h. At 230 °C, the Cu_6Sn_5 and Cu_5Zn_8 phases formed in Sn-20In-*x*Zn/Cu couples when $x \leq 0.7$ and $x \geq 1.0$, respectively

Cu couples reacted at 260 °C for 30 min, 2, and 6 h, and Sn-20In-2.0Zn/Cu couple reacted at 260 °C for 2 h, respectively. As shown in Fig. 2a, scallop-type IMC layers were found in the 0.7 wt%Zn-doped couple. Its composition was determined to be Sn-53.7 at.%Cu-6.9 at.%Zn-8.0 at.%In and the IMC layer was presumed to be the Cu_6Sn_5 phase with some In and Zn contents. Similar results were found in Sn-20In-0.5Zn/Cu couples reacted at 260 °C. For the 2.0 wt%Zn-doped couples, as shown in Fig. 2e, the IMC layer composed of smaller scallop-type grains was observed. According to its composition of Cu-66.0 at.%Zn, this IMC layer was presumed to be the Cu_5Zn_8 phase without detectable In and Sn contents. Similar results were found in Sn-20In-3.0Zn/Cu couples reacted at 260 °C. These results of interfacial reactions in 0.5, 0.7, 2.0, and 3.0 wt%Zn-doped couples reacted at 260 °C are all similar to those in couples reacted at 230 °C. Both Cu_6Sn_5 and Cu_5Zn_8 phases were formed when Zn doping level $\leq$0.7 and $\geq$2.0 wt%, respectively, as summarized in Table 1.

The reactions in 0.5, 0.7, 2.0, and 3.0 wt%Zn-doped couples reacted at 260 °C were similar to those in couples reacted at 230 °C; however, the reactions changed drastically in 1.0 wt%Zn-doped couples, i.e., Sn-20In-1.0Zn/Cu, reacted at 260 °C. As shown in Fig. 2b, after a 30-min reaction at 260 °C, a loose IMC layer was formed at the interface. Its composition was determined to be Cu-40.8 at.%Zn-5.8 at.%Sn-2.4 at.%In. Since In and Sn have similar atomic sizes and crystallographic properties, great mutual solubility between Cu–In and Cu–Sn compounds has been found in the Cu–In–Sn ternary system [7, 17]. Therefore, the contents of In and Sn were considered together as the Sn content and the IMC layer was presumed to be the CuZn phase with 2.4 wt%In and 5.8 wt%Sn according to the Cu–Sn–Zn 250 °C isothermal section [18]. When the reaction time was increased to 2 h, the CuZn layer grew thicker and became denser, as shown in Fig. 2c. In addition, a bright thin layer could be found between the previously formed CuZn layer and the Cu substrate. The composition of the newly formed bright IMC layer was determined to be Cu-21.5 at.%Zn-17.8 at.%Sn-5.6 at.%In. For similar reasoning mentioned above, the Cu–Sn–Zn phase equilibria were employed with the Sn content taken from the combined contents of In and Sn; however, it falls

Table 1 Summary of reaction products between the Sn-20.0 wt% In-*x* wt% Zn solders with Cu, Ni, or Ag substrates reacted at 230, 260, or 150 °C

Reaction temperature (°C)	Couple type	Doping level (wt%)	Interfacial phases
230	L/S	$x = 0.5, 0.7$	Cu_6Sn_5[a]
		$x = 1.0, 2.0, 3.0$	Cu_5Zn_8[a]
260	L/S	$x = 0.5, 0.7$	Cu_6Sn_5[a]
		$x = 1.0$	CuZn (initially)
			CuZn/ CuZn + Cu_6Sn_5[a]
		$x = 2.0, 3.0$	Cu_5Zn_8[a]
150	S/S	$x = 0.5$	Cu_6Sn_5[a]
		$x = 0.7$	CuZn/Cu_6Sn_5 (as-jointed)
			Cu_6Sn_5/CuZn/ Cu_6Sn_5 (transient)
			Cu_6Sn_5[a]
		$x = 1.0$	Cu_6Sn_5/Cu_5Zn_8/ Cu_6Sn_5 or
			Cu_5Zn_8/Cu_6Sn_5 (transient)
			Cu_6Sn_5[a]
		$x = 2.0$	Cu_5Zn_8/Cu_6Sn_5 or
			Cu_5Zn_8/solder/ Cu_6Sn_5[a]
		$x = 5.0$	Cu_5Zn_8[a]

[a] Terminal phase(s) in the couples for the time scale of observation in the study

within the CuZn + Cu_6Sn_5 two-phase region. In order to identify the phase, the reaction was prolonged to 6 h for a larger reaction zone. As shown in Fig. 2d, the thickness of the CuZn layer did not increase much, but the bright layer grew thicker. As shown in the magnified image in Fig. 2d, the bright phase is composed of fine dark grains embedded in a bright matrix. Therefore, the dark grains and bright matrix are presumed to be the CuZn and Cu_6Sn_5 phases, respectively. As a result, the diffusion path across the interface is liquid/CuZn/Cu in the initial stage of reaction and then transforms to liquid/CuZn/CuZn + Cu_6Sn_5/Cu after a longer reaction time in Sn-20In-1.0Zn/Cu couples reacted at 260 °C. The Zn-doping effect upon Sn-20In-*x*Zn/Cu interfacial reactions at 260 °C is summarized in Table 1.

Interfacial reactions in Sn-20In-*x*Zn/Cu couples reacted at 150 °C

Figure 3 shows the BEI micrograph of the Sn-20In-0.5Zn/Cu couple reacted at 150 °C for 480 h. Prior to the solid-state ageing, a thin IMC layer has been found at the interface due to the fast reaction between Sn–In–Zn solders and Cu substrates. The IMC formed at the early stage of reactions is presumed to be the Cu_6Sn_5 phase with 14 at.%In and 4 at.%Zn according to its composition of Cu-26 at.%Sn-14 at.%In-4 at.%Zn. The thickness of the Cu_6Sn_5 layer increased with longer ageing time, such as the 480 h-reacted couple shown in Fig. 3. In addition, the Zn content in the Cu_6Sn_5 layer gradually changed from 4 wt% near the solder to 12 wt% adjacent to the Cu substrate, indicating that Zn is likely the dominant diffusion species towards the Cu substrate in the Cu_6Sn_5 layer.

Figure 4a–e shows the BEI micrographs of the as-jointed Sn-20In-0.7Zn/Cu couple, and the couples reacted at 150 °C for 5, 18, 50, and 600 h, respectively. As shown in Fig. 4a, two thin IMC layers had been formed prior to solid-state reactions for the 0.7 wt%Zn-doped couple. According to compositional analyses, the dark and bright IMC layers are presumed to be the CuZn phase with 9.6 at.%Sn and 3.0 at.%In and the Cu_6Sn_5 phase with 14.0 at.%In and 6.0 at.%Zn, respectively. The reaction phases across the interface were initially solder/CuZn/Cu_6Sn_5/Cu in Sn-20In-0.7Zn/Cu couples. After a 5-h reaction at 150 °C, as shown in Fig. 4b, the Cu_6Sn_5 layer grew thicker and part of the CuZn layer grew thicker as well, while the other part remained a thin layer with new Cu_6Sn_5 layer formed at the opposite side of the CuZn layer. As shown in Fig. 4c, when the reaction time was increased to 18 h, the CuZn layer became very thin and the interface became a Cu_6Sn_5/CuZn/Cu_6Sn_5 sandwich structure. With even longer reaction time of 50 h, the entire IMC became a single Cu_6Sn_5 layer, as shown in Fig. 4d. With further prolonged reaction up to 600 h, the Cu_6Sn_5 layer was still the only IMC at the interface, as shown in Fig. 4e.

Figure 5a–d shows the BEI micrographs of the Sn-20In-1.0Zn/Cu couples reacted at 150 °C for 120, 240, 480, and 600 h, respectively. No noticeable IMC could be found in the as-jointed Sn-20In-1.0Zn/Cu couple. After a 120-h reaction at 150 °C, several special features can be found at the interface. According to compositional analyses; they are (i) solder/Cu_6Sn_5/Cu_5Zn_8/Cu, (ii) solder/Cu_5Zn_8/Cu_6Sn_5/Cu, and (iii) solder/Cu_6Sn_5/Cu_5Zn_8/Cu_6Sn_5/Cu, as indicated by arrows in Fig. 5a. Similar solder/Cu_6Sn_5/Cu_5Zn_8/Cu_6Sn_5/Cu interfacial phase sequence has also been reported in Sn-9Zn-3Bi/Cu interfaces reacted at 170 °C [20]. When reaction time was increased to 240 h, in addition to the three types of interfacial phase sequence in the 120-h-reacted couple, two other feathers were found. They are (iv) solder/Cu_5Zn_8/solder/Cu_6Sn_5/Cu and (v) solder/Cu_6Sn_5/Cu, as indicated by arrows in Fig. 5b. When reaction time was further increased to 480 and 600 h, the entire interfaces became the combination of types (iii) and (v), as shown in Fig. 5c and d, respectively; that is, solder/

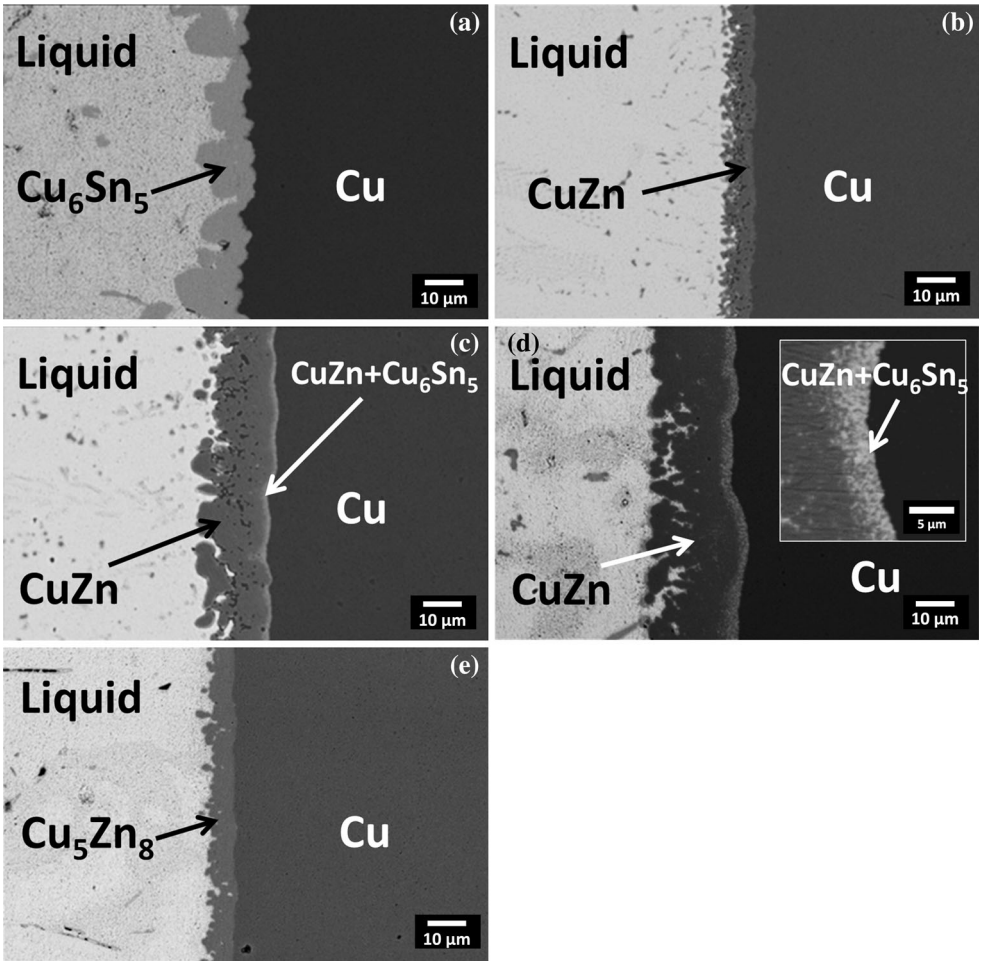

Fig. 2 BEI micrographs of the Sn-20In-*x*Zn/Cu couples reacted at 260 °C: **a** $x = 0.7$ for 2 h, **b** $x = 1.0$ for 30 min, **c** $x = 1.0$ for 2 h, **d** $x = 1.0$ for 6 h, and **e** $x = 2.0$ for 2 h. At 260 °C, the Cu_6Sn_5 and Cu_5Zn_8 phases formed in Sn-20In-*x*Zn/Cu couples when $x \leq 0.7$ and $x \geq 2.0$, respectively, while the transient CuZn phase formed when $x = 1.0$

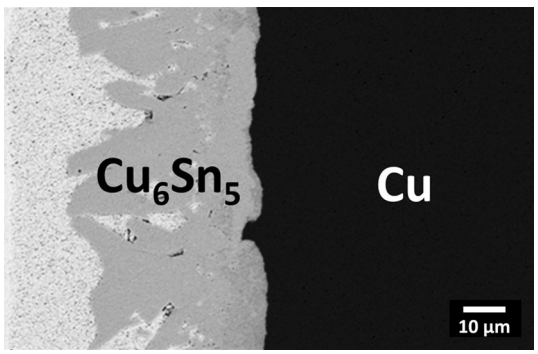

Fig. 3 BEI micrograph of the Sn-20In-0.5Zn/Cu couple reacted at 150 °C for 480 h. The Cu_6Sn_5 phase formed in Sn-20In-0.5Zn/Cu couples reacted at 150 °C

$Cu_6Sn_5/Cu_5Zn_8/Cu_6Sn_5/Cu$ where the Cu_5Zn_8 layer was discontinuous at some regions. Figure 6a–c shows the BEI micrographs of the Sn-20In-2.0Zn/Cu couples reacted at 150 °C for 50, 120, 240, and 600 h, respectively. Similar to the result in the as-jointed Sn-20In-1.0Zn/Cu couple, no noticeable IMC could be found in the as-jointed Sn-20In-2.0Zn/Cu couple. After a 50-h reaction at 150 °C, two types of interfacial morphology can be found. They are (i) solder/Cu_5Zn_8/Cu_6Sn_5/Cu and (ii) solder/Cu_5Zn_8/solder/Cu_6Sn_5/Cu, as shown in Fig. 6a. With longer reaction time up to 600 h, both type (i) and (ii) interfaces remained and the Cu_6Sn_5 layer grew thicker, as shown in Fig. 6b–c.

Figure 7 shows the BEI micrograph of the Sn-20In-5.0Zn/Cu couple reacted at 150 °C for 600 h, respectively. No noticeable IMC could be found in the as-jointed Sn-20In-5.0Zn/Cu couple. After reactions at 150 °C, only one Cu_5Zn_8 layer formed at the interfaces and the Cu_5Zn_8 layer grew thicker with longer reaction time, as shown in Fig. 7. The reaction phase formation in Sn-20In-*x*Zn/Cu couples with Zn doping levels of 0.5, 0.7, 1.0, 2.0, 5.0 wt% are summarized in Table 1. The interfacial reactions and microstructural evolution in the solid-state reactions are much more complicated than those in L/S couples. The reaction mechanisms, diffusion paths, phase transformation, and microstructural evolution of both the L/S and S/S Sn-20In-*x*Zn/Cu reactions will be discussed in the following sections.

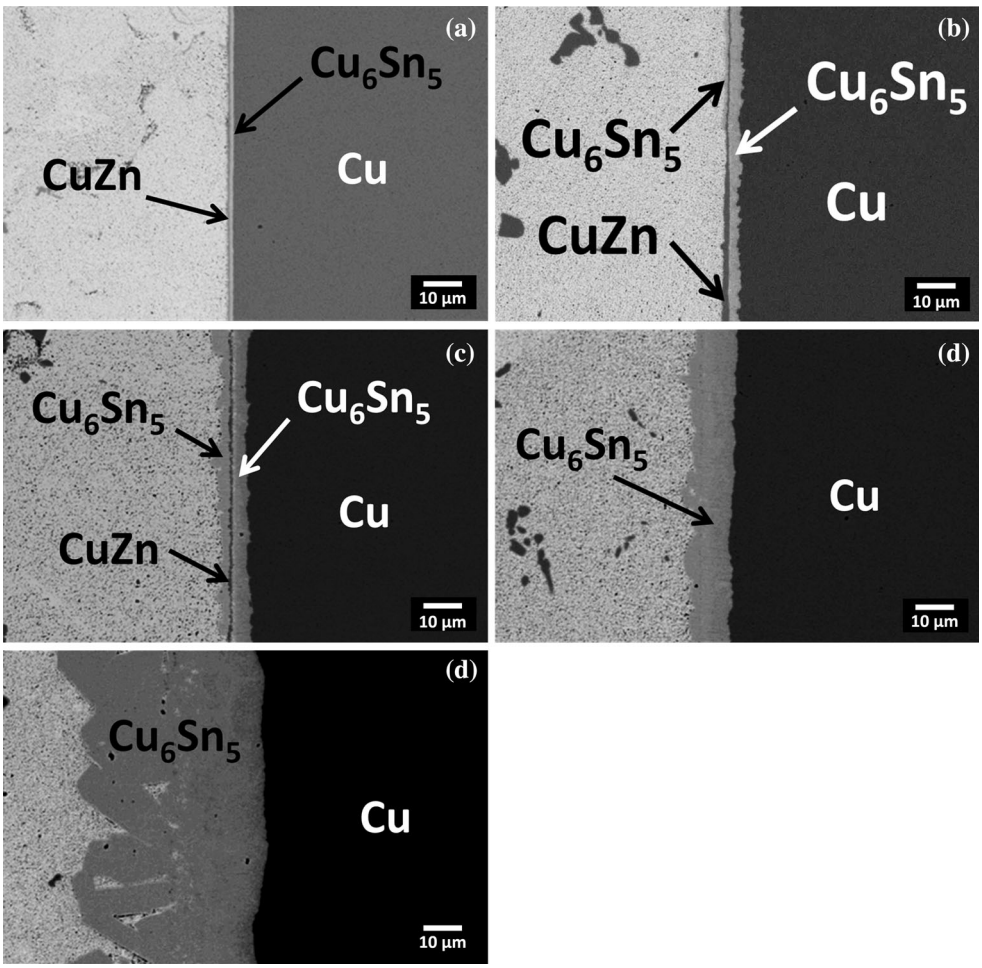

Fig. 4 BEI micrographs of the Sn-20In-0.7Zn/Cu couples reacted at 150 °C: **a** as-jointed (30 s at 230 °C), and for **b** 5 h, **c** 18 h, **d** 50 h, and **e** 600 h. The CuZn and Cu_6Sn_5 phases formed in Sn-20In-0.7Zn/Cu couples reacted at 150 °C, while the CuZn phase transformed into the Cu_6Sn_5 phase for longer reaction time

Discussion

Reaction mechanisms of the L/S Sn-20In-*x*Zn/Cu reactions

Figure 8a shows the schematic Cu–In–Sn–Zn isothermal tetrahedron at 250 °C [17, 18]. As summarized in Table 1, the IMCs formed at Sn-20In-*x*Zn/Cu interfaces at 150, 230, and 260 °C are either quaternary Cu–Sn compounds with some In and Zn contents or binary Cu–Zn compounds. As shown in Fig. 8b, the homogeneity ranges of Cu–Sn compounds in the Cu–In–Sn ternary system are generally in parallel with the Sn–In binary boundary, which indicates that In substitutes Sn in the ternary Cu–Sn compounds. Hence, when Cu–Sn compounds were the predominated reaction products, the combined Sn and In content in these quaternary Cu–Sn compounds can be considered together as the Sn content in Cu–Sn–Zn phase equilibria. On the other hand, when binary Cu–Zn compounds were the predominated reaction products, Sn and In do not participate in the reactions and thus the Cu–Sn–Zn phase equilibria can naturally be employed. Therefore, the Cu–Sn–Zn isothermal sections can be used for evaluating the Sn-20In-*x*Zn/Cu reactions.

The diffusion paths of the L/S Sn-20In-*x*Zn/Cu reactions are superimposed on the 250 °C isothermal section of the Cu–Sn–Zn ternary system as shown in Fig. 8c [18]. When the Zn doping level is $0.5 \leq x \leq 0.7$, the Cu_6Sn_5 phase is the predominated reaction phase for reactions at both 230 and 260 °C and the diffusion path is liquid/Cu_6Sn_5/Cu, which is similar to the results of Sn-20In/Cu reactions [8, 9]. When the Zn doping level is $1.0 \leq x \leq 3.0$ for reactions at 230 °C and $2.0 \leq x \leq 3.0$ for reactions at 260 °C, the Cu_5Zn_8 phase is the predominated reaction phase and the diffusion path is liquid/Cu_5Zn_8/Cu. It is clear that the IMC formation was the results of the competition between Cu–Sn and Cu–Zn reactions; i.e., when Zn doping level is high, Cu–Zn reactions dominate and when Zn doping level is low, Cu–Sn reactions dominate. Between the two extremes, e.g., the Sn-20In-1.0Zn/Cu reactions at 260 °C shown in Fig. 2b, the supplement of Zn was not sufficient for the formation of the Cu_5Zn_8 phase and the local equilibrium at liquid/Cu interface was shifted to the CuZn phase,

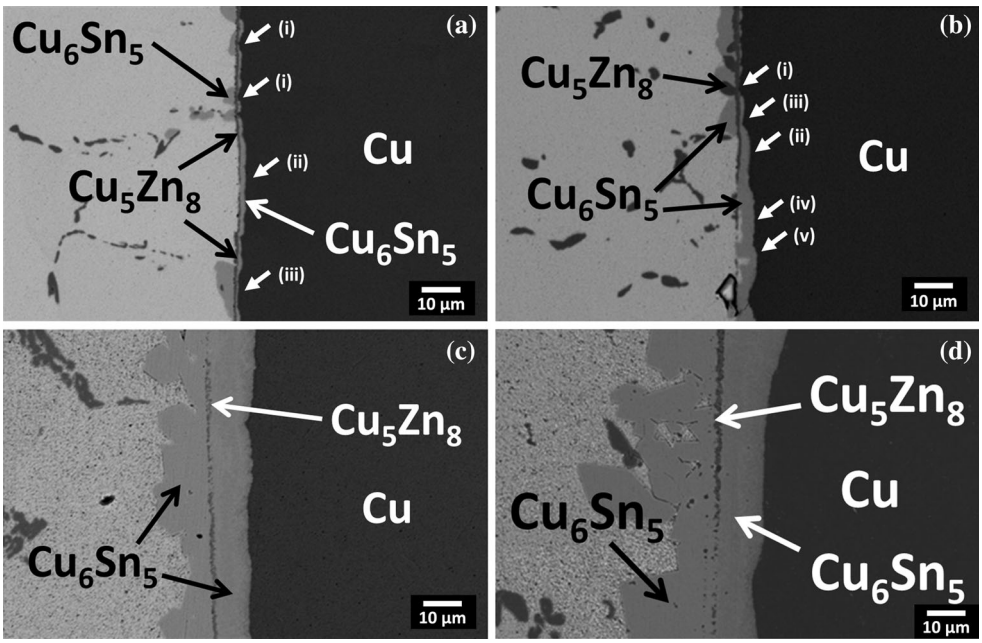

Fig. 5 BEI micrographs of the Sn-20In-1.0Zn/Cu couples reacted at 150 °C for **a** 120 h, **b** 240 h, **c** 480 h, and **d** 600 h. Five types of interfacial phase formed at interface of Sn-20In-1.0Zn/Cu couples reacted at 150 °C. They are *i* solder/Cu_6Sn_5/Cu_5Zn_8/Cu, *ii* solder/Cu_5Zn_8/Cu_6Sn_5/Cu, *iii* solder/Cu_6Sn_5/Cu_5Zn_8/Cu_6Sn_5/Cu, *iv* solder/Cu_5Zn_8/solder/Cu_6Sn_5/Cu, and *v* solder/Cu_6Sn_5/Cu. The Cu_5Zn_8 phase transformed into the Cu_6Sn_5 phase for longer reaction time

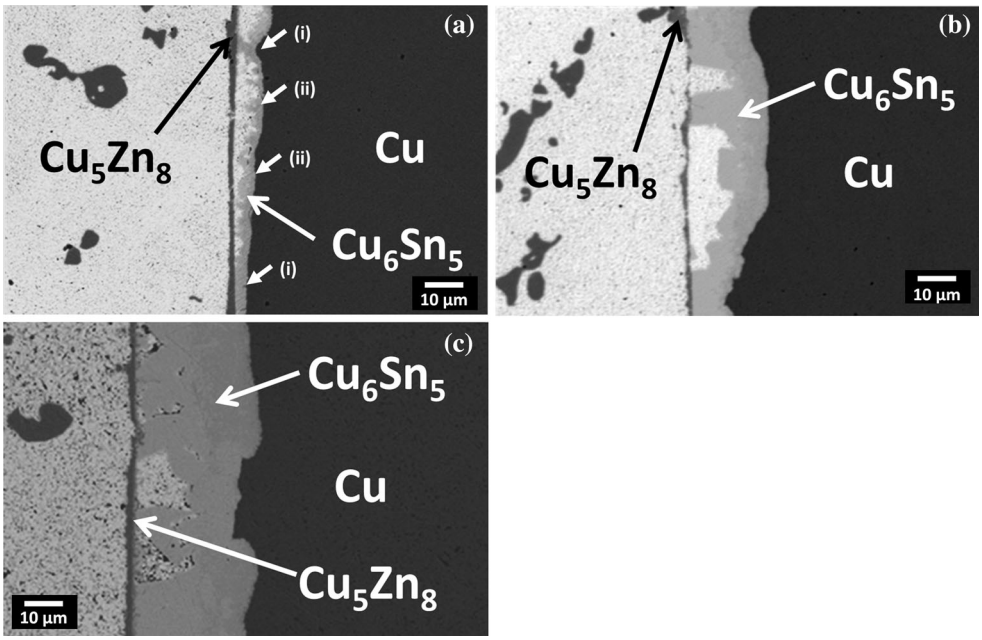

Fig. 6 BEI micrographs of the Sn-20In-2.0Zn/Cu couples reacted at 150 °C for **a** 50 h, **b** 240 h, and **c** 600 h. Two types of interfacial phase formed at interface of Sn-20In-2.0Zn/Cu couples reacted at 150 °C. They are *i* solder/Cu_5Zn_8/Cu_6Sn_5/Cu and *ii* solder/Cu_5Zn_8/solder/Cu_6Sn_5/Cu

which has less Zn content, and the diffusion path became liquid/CuZn/Cu, as shown in Fig. 8c. For longer reaction times, upon the depletion of Zn in the molten solder and the formation of the CuZn phase at the interface, the local equilibrium at CuZn/Cu interface was broken. The Cu_6Sn_5 phase was formed via the reaction CuZn + Sn + In + Cu = Cu_6Sn_5 and resulted in the CuZn + Cu_6Sn_5 two-phase layer between the CuZn layer and Cu substrate, as shown in Fig. 2c–d.

It can be concluded that in the L/S Sn-20In-*x*Zn/Cu reactions, the Cu_5Zn_8 phase is the reaction product when Zn doping level is high, the Cu_6Sn_5 phase is the reaction product when Zn doping level is low, and the transient CuZn phase forms when the Zn doping level is between the two critical values. These critical Zn doping levels depend on reaction temperatures as well as the chemical compositions of major contents of solders. The critical window of Zn doping levels that causes formation of the transient CuZn are around $1.0 < x < 2.0$ for Sn-20In-*x*Zn/Cu reactions at 230 °C, around $0.7 < x < 2.0$ for Sn-20In-*x*Zn/Cu reactions at 260 °C, around $0.5 < x < 2.0$ for Sn-*x*Zn/Cu reactions at 250 °C [21], and around $1.0 < x < 1.5$ for Sn-

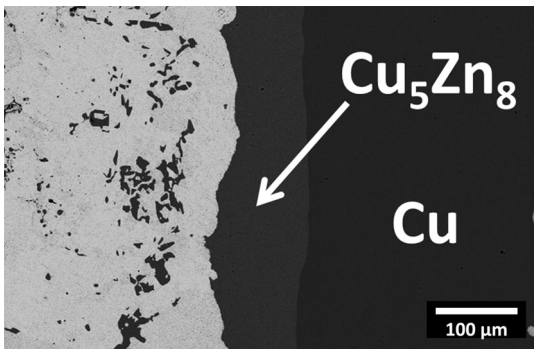

Fig. 7 BEI micrograph of the Sn-20In-5.0Zn/Cu couple reacted at 150 °C for 600 h. The Cu_5Zn_8 phase formed in Sn-20In-5.0Zn/Cu couples reacted at 150 °C

3.5Ag-0.7Cu -*x*Zn/Cu reactions at 260 °C [22]. Note that these critical windows are summarized based on a limited number of Zn doping levels being conducted in the literatures. The actual ranges of the critical windows may be smaller for individual cases.

Reaction mechanisms of the S/S Sn-20In-*x*Zn/Cu reactions

The diffusion paths of the S/S Sn-20In-*x*Zn/Cu reactions are superimposed on the 180 °C isothermal section of the Cu–Sn–Zn ternary system as shown in Fig. 8d [18]. In the Sn-20In-0.5Zn/Cu couples, the Cu_6Sn_5 phase is the only reaction product and the diffusion path is solder/Cu_6Sn_5/Cu, as shown in Fig. 8d. The Zn dopants all incorporated with the Cu–Sn reaction forming the Cu_6Sn_5 phase. When the Zn doping level is increased to 0.7 wt%, the initial diffusion path is solder/CuZn/Cu_6Sn_5/Cu, but it shifts to solder/Cu_6Sn_5/CuZn/Cu_6Sn_5/Cu and ends up becoming solder/Cu_6Sn_5/Cu as that in Sn-20In-0.5Zn/Cu couples, as shown in Fig. 8d. These results indicate that (1) the growth front of the Cu_6Sn_5 layer was at the solder side and Cu was the dominant diffusion species across the CuZn layer; and (2) the CuZn phase was not a stable interfacial compound and it transformed to the Cu_6Sn_5 phase due to the depletion of Zn in the solder matrix in Sn-20In-0.7Zn/Cu couples.

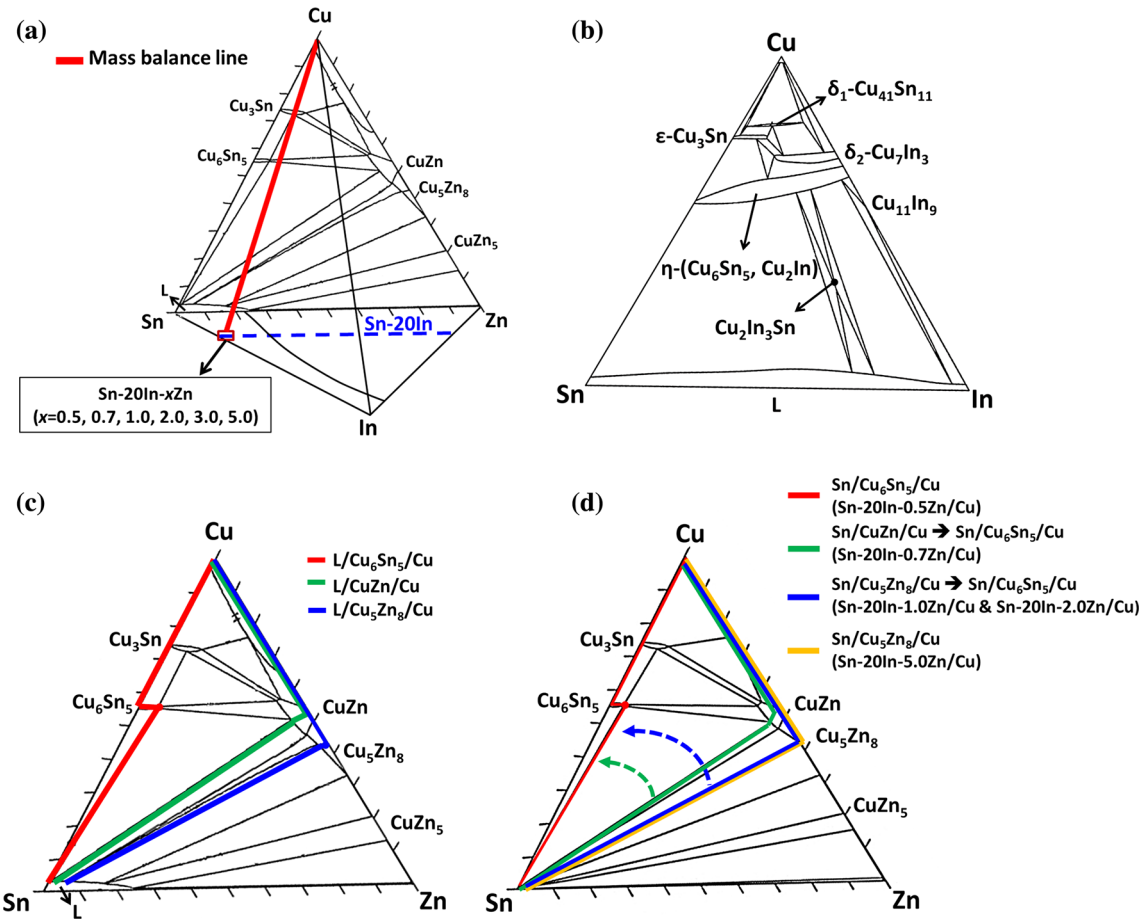

Fig. 8 **a** The schematic 250 °C isothermal tetrahedron of the Cu–In–Sn–Zn quaternary system; **b** the 250 °C isothermal section of the Cu–In–Sn ternary system [17]; and the isothermal section of the Cu–Sn–Zn ternary system at **c** 250 °C and **d** 180 °C [18] with diffusion paths superimposed

As presented in the "Results" section, there are five types of diffusion paths in the Sn-20In-1.0Zn/Cu couples as shown in Fig. 5, i.e., (i) solder/Cu_6Sn_5/Cu_5Zn_8/Cu, (ii) solder/Cu_5Zn_8/Cu_6Sn_5/Cu, (iii) solder/Cu_6Sn_5/Cu_5Zn_8/Cu_6Sn_5/Cu, (iv) solder/Cu_5Zn_8/solder/Cu_6Sn_5/Cu, and (v) solder/Cu_6Sn_5/Cu. According to morphological evolution at interfaces of the joints, the thin Cu_5Zn_8 layer is presumed to form first, so the Cu_5Zn_8/Cu contact could be found in type (i) regions. Owing to the formation of the Cu_5Zn_8 phase, the Zn content near the interface was depleted and the Cu_6Sn_5 phase formed subsequently. The growth of the Cu_6Sn_5 phase relied on the inter-diffusion of Cu from the substrate and Sn from the solder. Since the Cu_6Sn_5 phase was found in the solder side (type i), in the substrate side (type ii), and at both sides simultaneously (type iii) of the Cu_5Zn_8 layer, it was likely that the diffusion rates of Cu and Sn atoms were generally comparable and the growth fronts of the Cu_6Sn_5 layer was governed by the local diffusion pathways. The two Cu_6Sn_5 layers both grew thicker with longer reaction time; however, the Zn content in the Cu_6Sn_5 layers adjacent to the Cu substrate was higher (7 at.%), while that at the solder side was lower (3 at.%), indicating that Zn outflow from the Cu_5Zn_8 layer towards the Cu substrate participated in the growth of the Cu_6Sn_5 layers adjacent to the Cu substrate. Hence, the Cu_5Zn_8 phase gradually dissociated after longer reaction time. The joint would eventually become solder/Cu_6Sn_5/Cu at the interface of Sn-20In-1.0Zn/Cu couples reacted at 150 °C. Regardless the kinetics reasoning, the microstructural evolution can be comprehended with the diffusion path shifting from solder/Cu_6Sn_5/Cu_5Zn_8/Cu to solder/Cu_6Sn_5/Cu, as shown in Fig. 8d.

In the Sn-20In-2.0Zn/Cu couples, two types of diffusion paths in the Sn-20In-1.0Zn/Cu couples were found as shown in Fig. 6, i.e., (i) solder/Cu_5Zn_8/Cu_6Sn_5/Cu and (ii) solder/Cu_5Zn_8/solder/Cu_6Sn_5/Cu. The type (i) phase sequence is similar to one of the resultant morphologies in Sn-20In-1.0Zn/Cu couples reacted at 150 °C. Based on the discussion on Sn-20In-1.0Zn/Cu couples, it is likely the Cu_5Zn_8 phase also formed first between solder and Cu substrate. However, the Cu_6Sn_5 phase formed only at the substrate side of the Cu_5Zn_8 layer, indicating that Sn was the dominant diffusion species across the Cu_5Zn_8 layer, which acted as an effective diffusion barrier for Cu. However, the type (ii) phase sequence was rather peculiar, with the unreacted solder in the reaction diffusion zone between the two IMCs. The inflow of Sn and growth of the Cu_6Sn_5 phase in contact with Cu_5Zn_8 might have created stresses on the rigid Cu_5Zn_8 layer, or in the three-dimensional point of view, on the rigid Cu_5Zn_8 plan. The stresses upon the solder near the Cu_5Zn_8 plan would promote the inflow of mass towards the substrate. If the outflow of Cu was insufficient for Cu_6Sn_5 formation, Sn would then accumulate between the Cu_5Zn_8 and Cu_6Sn_5 phases. Therefore, the non-uniform interface with mixed type (i) and (ii) phase sequences would form. Although the diffusion path shifting in Sn-20In-1.0Zn/Cu and Sn-20In-2.0Zn/Cu couples is similar, as shown in Fig. 8d, comparing the results in these couples shows that thicker Cu_5Zn_8 layer formed in the early stage of reactions could stop the outward diffusion of Cu, as shown in Fig. 6, while Cu atoms could penetrate the thinner Cu_5Zn_8 layer, which would eventually dissociate within the Cu_6Sn_5 layer, as shown in Fig. 5.

In the Sn-20In-5.0Zn/Cu couples, the Cu_6Sn_5 phase no longer forms at the interface. The diffusion path is simply solder/Cu_5Zn_8/Cu, as shown in Fig. 8d. Not only Cu but also Sn was not able to penetrate the thick Cu_5Zn_8 layer. It is clear that the thickness of the Cu_5Zn_8 layer formed in the early stage of reactions is critical to the subsequent reactions and morphological evolution.

The interesting and sensitive interfacial morphology evolutions upon Zn doping levels were due to the two facts: (1) the high activity of Zn that Cu–Zn reactions dominate when Zn doping level is high; and (2) the limited supplements of Zn that depletion of Zn in solder breaks the local equilibrium between Cu–Zn compounds and Cu substrate and shifts diffusion paths. As shown in Fig. 8d, the diffusion path of Sn-20In-*x*Zn/Cu reaction evolves with Zn doping levels. It is solder/Cu_6Sn_5/Cu or solder/Cu_5Zn_8/Cu without shifting when Zn doping level is low enough ($x \leq 0.5$) or high enough ($x \geq 5.0$), respectively. For medium Zn doping levels, transient Cu–Zn compounds form, such as CuZn ($x = 1.0$) and Cu_5Zn_8 ($1.0 \leq x \leq 2.0$), and both of them will end up transforming into the Cu_6Sn_5 phase due to the depletion of Zn in solders.

Kinetics of interfacial reactions in Sn-20In-*x*Zn/Cu couples

Figure 9a shows the plot of IMC thickness as a function of Zn content in Sn-20In-*x*Zn/Cu couples reacted at 230 and 260 °C for 2 h. Although the reactions at 230 and 260 °C are both L/S reactions, the IMC thicknesses are not always thicker in the couples reacted at higher temperature. It is because the type of IMC has changed due to the slight difference in temperature (30 °C). For the reaction conditions that the Cu_6Sn_5 phase is the predominated reaction phase, i.e., Sn-20In-0.5Zn/Cu and Sn-20In-0.7Zn/Cu couples reacted at 230 and 260 °C, the Cu_6Sn_5 layers were all thicker in the couples with higher Zn contents. However, the IMCs were thinner for even higher Zn doping levels when the predominated reaction phase was changed to the Cu_5Zn_8 phase; i.e., when the Zn doping level is higher than 1.0 wt% and 2.0 wt% for reactions at 230 and 260 °C,

respectively, as summarized in Table 1. This is likely because the Cu_5Zn_8 phase was with approximately 65 at.%Zn and without detectable contents of Sn and In. Hence, it not only accommodates the segregated active Zn atoms without excess IMC growth, but also acts as a diffusion barrier between Cu and Sn or In. Nevertheless, the effects of Zn content upon the thicknesses of both Cu_6Sn_5 and Cu_5Zn_8 phases show the same trend; i.e., the higher the Zn contents were doped in the solders, the thicker the IMCs would be formed. The singular peak in Fig. 9a is the result of Sn-20In-1.0Zn/Cu reaction at 260 °C. Under such reaction condition, the predominated reaction phase is the CuZn phase. Although the CuZn phase contains about 40 at.%Zn, Sn and In also participate in the formation of the CuZn phase, leading to a faster IMC growth rate. During the Sn-20In-*x*Zn/Cu soldering process, proper amount of Zn doping that causes formation of a minimum amount of the Cu_5Zn_8 phase is desired. In summary, as shown in Fig. 9a, Sn-20In-1.0Zn/Cu and Sn-20In-2.0Zn/Cu showed superior IMC growth rate at 230 and 260 °C, respectively.

Figure 9b shows the plot of IMC thickness as a function of Zn content in Sn-20In-*x*Zn/Cu couples reacted at 150 °C for 120, 240, and 600 h. The thickness of the reaction layer formed depends strongly on the Zn content in the couples during solid-state thermal ageing. It is again ascribed to the type of IMC formation. As discussed in previous sections and summarized in Table 1, Cu_6Sn_5 and Cu_5Zn_8 phases were the only reaction phase for Sn-20In-0.5Zn/Cu and Sn-20In-5.0Zn/Cu couples, respectively. However, except for these two couples, the interfacial reactions in Sn-20In-0.7Zn/Cu, Sn-20In-1.0Zn/Cu, and Sn-20In-2.0Zn/Cu couples all involved transient stages with either the CuZn or Cu_5Zn_8 phase, which transformed to the Cu_6Sn_5 phase after prolonged reactions. As shown in Fig. 9b, with shorter reaction times of 120 and 240 h, the couple with the Cu_6Sn_5 phase as the only reaction phase, namely the Sn-20In-0.5Zn/Cu couple, showed the thickest IMC, while those involving Cu–Zn compounds had relatively thinner IMCs. The formation of Cu–Zn compounds suppressed the excess growth of the Cu_6Sn_5 phase. However, with prolonged reactions up to 600 h, the couple with the greatest Zn doping, namely the Sn-20In-5.0Zn/Cu couple, had the Cu_5Zn_8 phase as the only reaction product and showed drastically thicker IMC than those in the other couples with transient Cu–Zn IMC formation. It is likely that phase transition played an important role in mitigating IMC growth. In Sn-20In-0.7Zn/Cu couples, the CuZn phase formed first and transformed to the Cu_6Sn_5 phase with longer reaction times. However, it did not mitigate the interfacial reactions. As shown in Fig. 9b, among these couples with Cu–Zn IMCs, the 1.0 and 2.0 wt% Zn-doped solders showed the gentlest reactions with Cu. In these couples, the Cu_5Zn_8 phase formed first and detached from the Cu substrate due to the newly formed Cu_6Sn_5 phase and/or the inflow of Sn and In. Therefore, it can be concluded that in the Sn–In–Zn/Cu system, the Cu_5Zn_8 phase can act as the diffusion barrier and suppress the growth of the predominated Cu_6Sn_5 phase.

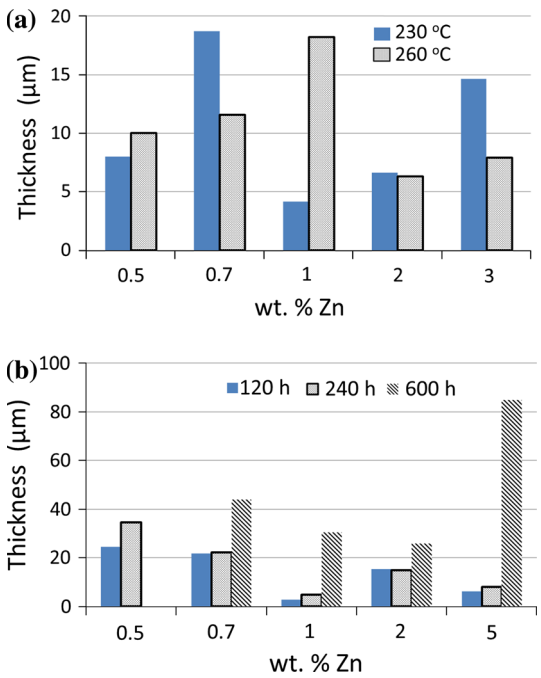

Fig. 9 Plots of IMC thickness in the Sn-20In-*x*Zn/Cu couples reacted at **a** 230 and 260 °C for 2 h and **b** 150 °C for 120, 240, and 600 h, respectively, as function of Zn content in wt%. 2 wt% was found to be the optimal Zn doping level for Sn-20In solders to bond with Cu substrate

Conclusions

Zn content has a significant effect on the reaction phase formation and interfacial microstructural evolution in Sn-20In-*x*Zn/Cu couples reacted at 150, 230, and 260 °C. The Cu_6Sn_5 phase forms in Sn-20In-*x*Zn/Cu couples with the following Zn doping levels: $x \leq 0.7$ for reactions at 230 and 260 °C and $x = 0.5$ for reactions at 150 °C, while the Cu_5Zn_8 phase forms in Sn-20In-*x*Zn/Cu couples with the following Zn doping levels: $1.0 \leq x \leq 3.0$ for reactions at 230 °C, $2.0 \leq x \leq 3.0$ for reactions at 260 °C, and $x = 5.0$ for reactions at 150 °C. Between the two extremes, the transient CuZn phase forms in Sn-20In-*x*Zn/Cu couples with $x = 1.0$ for reactions at 260 °C and $x = 0.7$ for reactions at 150 °C, while the transient Cu_5Zn_8 phase forms in Sn-20In-*x*Zn/Cu couples with $x = 1.0$ and 2.0 for reactions at 150 °C.

In summary, 2.0 wt%Zn is found to be an optimal amount for addition to the Sn-20In solder that can result in transient formation of the Cu_5Zn_8 phase in solid-state ageing without forming the undesired CuZn phase during soldering, and the Cu_5Zn_8 phase can suppress the growth of the predominated Cu_6Sn_5 phase.

Acknowledgements The authors acknowledge the financial support of National Science Council of Taiwan (NSC97-2221-E-007-067-MY3).

References

1. Suganuma K (2001) Advances in lead-free electronics soldering. Curr Opin Solid State Mater Sci 5:55–64
2. Chen S-W, Wang C-H, Lin S-K, Chiu C-N (2007) Phase diagrams of Pb-free solders and their related materials systems. J Mater Sci 18:19. doi:10.1007/s10854-006-9010-x
3. The Restriction of Hazardous Substances in Electrical and Electronic Equipment (ROHS), Official Journal of the European Union: L 37/19-L 37/23
4. Abtew M, Selvaduray G (2000) Lead-free solders in microelectronics. Mat Sci Eng R 27:95–141
5. Zeng K, Tu KN (2002) Six cases of reliability study of Pb-free solder joints in electronic packaging technology. Mat Sci Eng R 38:55–105
6. Laurila T, Vuorinen V, Kivilahti JK (2005) Interfacial reactions between lead-free solders and common base materials. Mat Sci Eng R 49:1–60
7. Lin S-K, Yang C-F, Wu S-H, Chen S-W (2008) Liquidus projection and solidification of the Sn–In–Cu ternary alloys. J Electron Mater 37:498–506
8. Chen S-W, Lin S-K (2006) Electric current-induced abnormal Cu/gamma-$InSn_4$ interfacial reactions. J Mater Res 21:3065–3071
9. Lin S-K, Chen S-W (2006) Interfacial reactions in the Sn-20 at.% In/Cu and Sn-20 at.% In/Ni couples at 160 degrees C. J Mater Res 21:1712–1717
10. Chen S-W, Lin S-K (2006) Effects of temperature on interfacial reactions in gamma-$InSn_4$/Ni couples. J Mater Res 21:1161–1166
11. Huang C-Y, Chen S-W (2002) Interfacial reactions in In–Sn/Ni couples and phase equilibria of the In–Sn–Ni system. J Electron Mater 31:152–160
12. Lee CC, Choe S (2002) Fluxless In–Sn bonding process at 140 degrees C. Mater Sci Eng A 333:45–50
13. Chen S-W, Hsu C-W, Lin S-K, Hsu C-M (2013) Reaction evolution in Sn-20.0 wt% In-2.8 wt% Ag/Ni couples. J Mater Res 28:3257–3260
14. Lin S-K, Hsu C-W, Chen S-W, Hsu C-M (2013) Interfacial reactions in Sn-20In-2.8Ag/Cu couples. Mater Chem Phys 142:268–275
15. Jee YK, Ko YH, Yu J (2007) Effect of Zn on the intermetallics formation and reliability of Sn-3.5Ag solder on a Cu pad. J Mater Res 22:1879–1887
16. Cho MG, Kang SK, Shih DY, Lee HM (2007) Effects of minor additions of Zn on interfacial reactions of Sn–Ag–Cu and Sn–Cu solders with various Cu substrates during thermal aging. J Electron Mater 36:1501–1509
17. Lin S-K, Chung T-Y, Chen S-W, Chang C-H (2009) 250 degrees C isothermal section of ternary Sn–In–Cu phase equilibria. J Mater Res 24:2628–2637
18. Chou C-Y, Chen S-W (2006) Phase equilibria of the Sn–Zn–Cu ternary system. Acta Mater 54:2393–2400
19. Miodownik AP (1990) Cu–Zn. In: Massalski TB, Okamoto H (eds) Binary alloy phase diagrams, 2nd edn. ASM International, Materials Park, pp 1508–1510
20. Duan LL, Yu DQ, Han SQ, Ma HT, Wang L (2004) Microstructural evolution of Sn-9Zn-3Bi solder/Cu joint during long-term aging at 170 degrees C. J Alloy Compd 381:202–207
21. Yang SC, Ho CE, Chang CW, Kao CR (2006) Strong Zn concentration effect on the soldering reactions between Sn-based solders and Cu. J Mater Res 21:2436–2439
22. Kotadia HR, Mokhtari O, Clode MP, Green MA, Mannan SH (2012) Intermetallic compound growth suppression at high temperature in SAC solders with Zn addition on Cu and Ni–P substrates. J Alloy Compd 511:176–188